ARL-TR-8604 • JAN 2019

US Army Research Laboratory

Safety Considerations for UV-C LED Applications

by Hakan Arslan, Fikadu T Dagefu, Robert J Drost, and Michael J Weisman

NOTICES

Disclaimers

The findings in this report are not to be construed as an official Department of the Army position unless so designated by other authorized documents.

Citation of manufacturer's or trade names does not constitute an official endorsement or approval of the use thereof.

Destroy this report when it is no longer needed. Do not return it to the originator.

ARL-TR-8604 ● JAN 2019

US Army Research Laboratory

Safety Considerations for UV-C LED Applications

by Hakan Arslan, Fikadu T Dagefu, Robert J Drost, and Michael J Weisman
Computational and Information Sciences Directorate, ARL

REPORT DOCUMENTATION PAGE

Form Approved
OMB No. 0704-0188

PLEASE DO NOT RETURN YOUR FORM TO THE ABOVE ADDRESS.

1. REPORT DATE *(DD-MM-YYYY)*	2. REPORT TYPE	3. DATES COVERED (From - To)
January 2019	Technical Report	January 2017–October 2017

4. TITLE AND SUBTITLE
Safety Considerations for UV-C LED Applications

5a. CONTRACT NUMBER

5b. GRANT NUMBER

5c. PROGRAM ELEMENT NUMBER

6. AUTHOR(S)
Hakan Arslan, Fikadu T Dagefu, Robert J Drost, and Michael J Weisman

5d. PROJECT NUMBER
R.0022661.4

5e. TASK NUMBER

5f. WORK UNIT NUMBER

7. PERFORMING ORGANIZATION NAME(S) AND ADDRESS(ES)
US Army Research Laboratory
ATTN: RDRL-CIN-T
Adelphi, MD 20783-1138

8. PERFORMING ORGANIZATION REPORT NUMBER
ARL-TR-8604

9. SPONSORING/MONITORING AGENCY NAME(S) AND ADDRESS(ES)

10. SPONSOR/MONITOR'S ACRONYM(S)

11. SPONSOR/MONITOR'S REPORT NUMBER(S)

12. DISTRIBUTION/AVAILABILITY STATEMENT
Approved for public release; distribution is unlimited.

13. SUPPLEMENTARY NOTES
<robert.j.drost6.civ@mail.mil>

14. ABSTRACT
In this report, we calculate the ultraviolet (UV) exposure limits when working with incoherent artificial UV radiation sources designed for communication links at UV-C band. Limits for adjacent bands can be calculated based on the approach described. The results are obtained based on the regulations established by independent organizations, such as the International Commission on Non-Ionizing Radiation Protection, the International Electrotechnical Commission, and the International Labour Organization.

15. SUBJECT TERMS
Ultraviolet communications, safety, exposure limits, power, line-of-sight measurements

16. SECURITY CLASSIFICATION OF:			17. LIMITATION OF ABSTRACT	18. NUMBER OF PAGES	19a. NAME OF RESPONSIBLE PERSON
a. REPORT	b. ABSTRACT	c. THIS PAGE			Robert J Drost
Unclassified	Unclassified	Unclassified	UU	37	19b. TELEPHONE NUMBER (Include area code) 301-394-0158

Standard Form 298 (Rev. 8/98)
Prescribed by ANSI Std. Z39.18

Contents

List of Figures

List of Tables

1. Introduction

The potential use of the ultraviolet (UV) spectrum for moderate rate covert communications for both line-of-sight (LOS) and non-line-of-sight (NLOS) scenarios has recently been investigated.[1,2] Recent advances in semiconductor UV sources and detectors, such as UV light-emitting diodes (LEDs) and avalanche photodiodes, will contribute to the realization of power efficient, small-size, low-cost, short-range wireless communication links at UV-C band[3,4]. These advances in component technologies also enable the development of compact modules appropriate for small gimbal systems and robotic platforms with which experimentation including channel modeling and multi-node networking can be conducted.

In addition to its potential benefits, UV radiation (UVR) is also known to cause severe health problems in humans. Because of the high photon energy and high absorption coefficient of human DNA at UV band, UV safety is a general public concern. Most people are familiar with potential health hazards associated with sun exposure, hence the use of sunscreen. The organs most vulnerable to damage from UVR are the skin and the eyes. Some acute and chronic effects due to UVR include but are not limited to development of non-melanoma skin cancer, skin aging, corneal injury, and cataracts[5]. Therefore, the effects of UV emitters in an experimental system should be fully understood in terms of maximum allowable exposure time as a function of distance from the source and time of exposure to ensure the safety of the operator and others within range of the transmitter.

This report aims to identify the UV exposure limits when working with incoherent artificial UVR sources designed for communication links at UV-C band. Limits for adjacent bands can be calculated based on the approach described. The results are obtained based on the regulations established by independent organizations, such as the International Commission on Non-Ionizing Radiation Protection (ICNIRP), the International Electrotechnical Commission (IEC), and the International Labour Organization (ILO).

Potential damage due to UV radiation is determined by the power and duration of the radiation incident upon a given area of the body as well as the geometry of the exposure[6]. In this report, we consider the worst case scenario, when radiation is directed perpendicularly to the surface of the skin or eye.

In general, the exposure limits (ELs) for skin can vary based on skin type, whereas UV sensitivity of ocular media is considered to be the same among individuals. It is understood that the highest sensitivity skin type (melano-compromised) and ocular media have the same degree of sensitivity[7]— hence, the same level of UV ELs. To compute a threshold level for safe operation (e.g., maximum allowable UV exposure time), we focus on exposure limits that are associated with ocular media (or equivalently, highest sensitivity skin type).

We find the maximum allowable UV exposure time (T_{max}), based on the limits associated with the eye for a particular system model, illustrated in Fig. 1. References are made to a particular system and its component devices being used at the US Army Research Laboratory (ARL), not only to document safety guidelines specifically associated with this system, but also as a guide facilitating the application of the general concepts to other systems and devices. In Fig. 1, a UV source radiates photons in a narrow beam in an LOS channel between the source and the detector. Potential multipath components have not been included in this analysis.

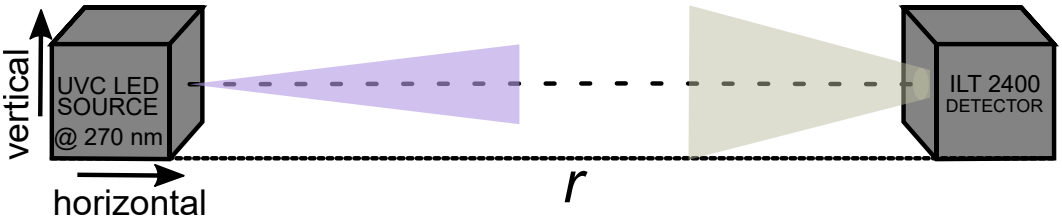

Fig. 1 A UV wireless communication model. The UV source can be modeled as a point source with directional narrow beam. The LOS channel represents the free-space loss between the UV source and UV detector.

In this study, we focus on the daily UV exposure limits for an off-the-shelf UV LED. The results depend on the features of the source, such as output power, spectral response, angular response, and peak wavelength, as well as the location of the subject's position with respect to the source. The subsequent sections discuss these features and assumptions in more detail. In Section 2, some background information about UV spectrum and UV sub-bands is given regarding the safety issues. In Section 3, the concept of effective irradiance and an analysis of calculating T_{max}, the maximum exposure time, are described. In Section 4, computations for exposure time limits for an actual UV LED source at UV-C band are presented.

2. General Information about UV Spectrum

The portion of the electromagnetic (EM) spectrum that lies between the visible light (VL) and the X-ray region is called the UV band, which includes wavelengths* from $10\,\mathrm{nm}$ to $400\,\mathrm{nm}$ (i.e., frequencies from $8 \times 10^{14}\,\mathrm{Hz}$ to $3 \times 10^{16}\,\mathrm{Hz}$). The ultraviolet band is divided into several sub-bands because UV radiation at different wavelengths exhibits different propagation characteristics in various media (e.g., the atmosphere, living tissues).[8] The UV-A band (long-wave UV) consists of radiation from 320 nm to 400 nm, the UV-B band (middle-wave UV) ranges from 290 nm to 320 nm, and the UV-C band (short-wave UV) spans 100 nm to 290 nm. Extreme UV (EUV) radiation has the highest energy of the UV sub-bands and ranges from 10 nm to 100 nm. The electromagnetic spectrum, which contains the UV bands, is shown in Fig. 2 and is categorized by wavelength, frequency, and energy. The wavelength and frequency are inversely related by the formula $\lambda\nu = c$, where λ is wavelength, ν is frequency, and c is the speed at which the electromagnetic energy travels in free space. The energy is proportional to the frequency: $E = h\nu$, where h is Planck's constant.

Most of the UV-band photons that are present on the Earth's surface originate at the Sun. Approximately 7% of the total energy emitted by the Sun corresponds to UVR. The remaining radiation from the Sun is made up of 44% visible light, and 49% infrared radiation[10]. Photons of solar radiation can interact with the constituents of the atmosphere at atomic and molecular scale. The type of interaction (e.g., reflection, absorption, scattering) is mainly determined by the photon energy and the chemical structure of the atoms and molecules available inside the propogating medium. For instance, UV photons undergo absorption and scattering inside the atmosphere due to aerosols and other molecules, such as N_2, and O_2, and the Chapman Cycle (the continuous generation and removal of O_2 and O_3 molecules)[11]. Most of the UV-B photons (90%) and almost all of the UV-C photons emitted by the Sun are filtered at the Stratosphere layer; hence, not all the photons emitted from the Sun can reach the Earth's surface[12]. Around 95% of the UVR photons that pass through the atmosphere are composed of UVA photons[13,14].

*In general, for frequencies above $100\,\mathrm{GHz}$, the wavelength scale (in free space) is used to define the boundaries of the EM spectrum.

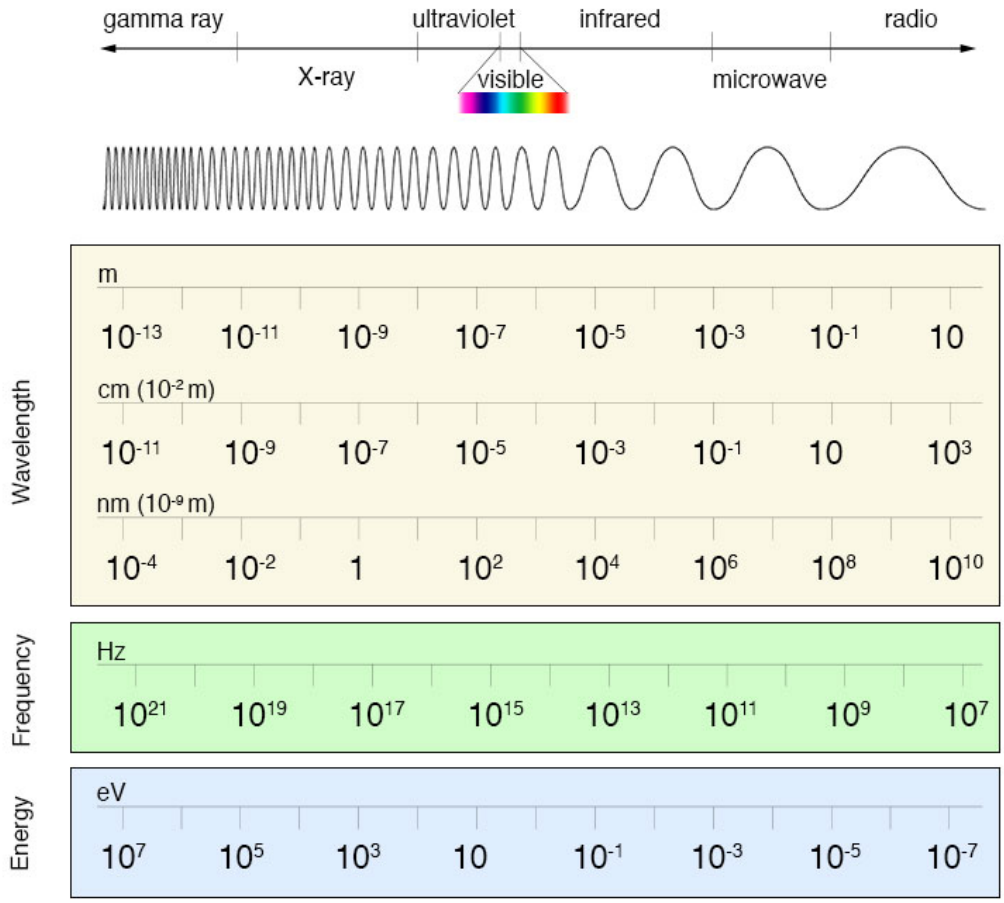

Fig. 2 The EM spectrum categorized by wavelength, frequency, and energy.[9] The UV band ranges from approximately 10 nm to approximately 400 nm and is divided into four sub-bands: UV-A, UV-B, UV-C, and EUV.

The actual transmission coefficient at a particular location depends on the position of the Earth with respect to the Sun (i.e., the time of the year and time of day), as well as other environmental factors, such as latitude, thickness, and concentration of the ozone layer, and the density of the clouds along the path of propagation[15–17].

Regarding the adverse effects on the human body, many studies show that high UV exposure at certain wavelengths can cause eyelid tumors, corneal and retinal injury, cataract formation[18,19], suppression of human immune system[20], and skin darkening (erythema, tanning), which can also trigger skin aging and can lead to skin cancer in the long term[21,22]; whereas insufficient exposure (for the epidermis layer of the skin) can cause lack of vitamin D synthesis[23,24] and, consequently, bone underdevelopment. Human DNA photodamage is another well known acute effect[25], especially at UV-C band[26]. Most of these effects depend on the radiation wavelength and become more significant at lower wavelengths. Figure 3 illustrates how body response changes with the wavelength of the radiation varying from 280 nm to 400 nm[24]. The lower limit on the chart was chosen because solar radiation below 280 nm is completely absorbed by the Earth's stratospheric ozone layer[24]. Human DNA, for example, becomes approximately 20,000 times more susceptible to damage from UV radiation when the wavelength drops from 320 nm to 280 nm.

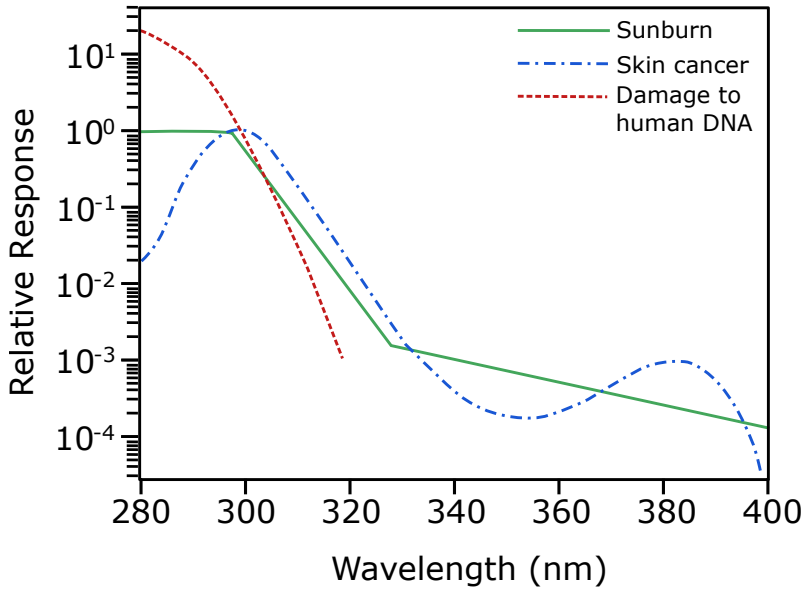

Fig. 3 Variations of the human body response level for sunburn, skin cancer, and DNA damage due to radiation at wavelengths in the range of 280–400 nm

This study is focused on time limits for UVR exposure emitted from an artificial narrow-band LED source at UV-C band (e.g., 270 nm–280 nm). Although the computed values significantly depend on the transmitter characteristics (such as peak wavelength, spectral power distribution, packaging, lens type, output power, etc.), the same approach can be applied to other UV transmitters to evaluate time limits.

The main source of UV-C band photons on the Earth's surface are emitted by man-made artificial sources[27], such as fluorescent UV sources, welding arcs, low pressure mercury-discharge (germicidal) lamps at $254\,\mathrm{nm}$, high-pressure metal-halide (xenon-filled flash) lamps (broad spectrum range), and narrow-band UV-C band LEDs. The contribution of solar radiation at the Earth's surface is almost negligible such that the interval between $230\,\mathrm{nm}$ and $290\,\mathrm{nm}$ of the spectrum is often referred to as "solar blind."

Skin and eyes exhibit higher degrees of biological sensitivity to UV-C radiation and some protective precautions must be taken while working with UV-C sources. Adverse effects of the UV-C band photons and some protective guidelines have been discussed in the literature[6,23,27,28]. Some restrictions have been established by ICNIRP to prevent individuals being exposed to excess amounts of UV-C radiation. These restrictions define the maximum irradiance limits during an 8-h period in a 24-h time window for the skin and eyes for each wavelength within the UV spectrum.

3. UV Exposure Limits for Safety Issues

Exposure limits (ELs) for both skin and ocular media are needed to guide the safe use of UV emitters. Our analysis follows the ICNIRP Guidelines[7], which also comply with the safety limits available in similar studies that have been published by other organizations such as the National Institute for Occupational Safety and Health (NIOSH) and the American Conference of Governmental Industrial Hygienists (ACGIH). The guidelines and regulations in these articles primarily reflect the concerns about skin and ocular media damage of individuals being exposed to UVR. The exposure limits have been developed with the aim of preventing any harmful changes in these organs. In addition, it is assumed that cellular recovery can take place and the associated damage is repaired after the exposure period has ended. The limits represent ceiling values for only the most sensitive skin type (melano-compromised) and ocular media for an exposure duration no longer than 8 hours in a 24-h cycle. For other skin types the limits can be exceeded, but we have not found any explicit quantitative data on this in the literature. In contrast to the skin, protection methods and safety limits of the eye remain the same for all individuals.

3.1 Figure of Merit: T_{max}

In this study, the ceiling values of ELs that are available in the references are used to calculate the safety limits. The figure of merit is *Maximum Exposure Time*, T_{max}, which is defined as the permissible exposure duration within an 8-h period per day such that UV exposure is considered to be safe and does not yield any adverse effects. The goal is to obtain T_{max} for artificial UV-C band sources to ensure the safety of the system operators. The value of T_{max} is characterized by the system parameters, including the UV emitter (e.g., power distribution across the spectrum), location of the receiver, surrounding objects that can lead to multi-path propagation of UVR, incident angle of the radiation upon receiver, and so on. Whenever one or more of these parameters is modified, T_{max} needs to be recalculated based on the new system topology and care should be taken by the individuals operating the equipment to protect themselves from an excess amount of UVR.

3.2 Exposure Limits

As mentioned in Section 2, radiation wavelength can have a significant impact on the degree of UVR hazard to human organs. Therefore, it is expected that ELs and T_{max} are functions of emission wavelength. In ICNIRP Guidelines[7], the UV exposure limits* are listed in a table for a substantial number of discrete wavelengths within the range of 180–400 nm (Table 1). For wavelength (λ) values that are not available in the table, ELs can be obtained by interpolating. The minimum EL ($3.0\,\mathrm{mJ/cm^2}$) is at $\lambda = 270\,\mathrm{nm}$. Therefore, radiation at a wavelength of $270\,\mathrm{nm}$ is considered most hazardous for the human body, which also indicates that the permissible exposure duration at this wavelength is shortest with all other parameters the same.

ELs range from $30\,\mathrm{Jm^{-2}}$ (at $270\,\mathrm{nm}$) to 1 million $\mathrm{Jm^{-2}}$ (at $400\,\mathrm{nm}$). With such a high dynamic range among the ELs, one could expect a similar distribution for T_{max} throughout the band, which also delineates the importance of calculations of T_{max} for safety concerns while working with the emitters that are operating in the close vicinity of the most sensitive region (i.e., UV-C band). Depending on the spectral distribution function of the UV source, several minutes could be long enough to exceed the daily allowed dose for an individual who is, for example, 3 ft away from the emitter. In fact, accurate calculations of T_{max} require an advanced modeling of the entire system (such as multi-path radiation patterns due to the reflections and scattering—which is, in general, hard to achieve) and full characterization of the UV source.

Other than the ELs given in Table 1, there are additional restrictions that apply mostly for UV-A band radiation. According to the ICNIRP Guidelines[7], the maximum allowed radiant exposure upon an unprotected ocular media due to incoherent UV sources within the band of 315–400 nm is $1\,\mathrm{J/cm^2}$. Of primary concern is the prevention of any photochemical reactions inside the ocular region due to long-term exposures. Moreover, for exposure durations greater than $1\,\mathrm{s}$ the irradiance level at the receiver must be below $10^3\,\mathrm{mW/cm^2}$ to avoid thermal damage for both skin and eye. Note that ELs available in the table at UV-B/UV-C band wavelengths are more conservative than these additional restrictions. Lastly, these ELs do not apply for laser sources.

*The dimension of Exposure Limit (EL) is energy per unit area.

Table 1 UV ELs for a monochromatic source and spectral weighting function $S(\lambda)$. Reproduced from ICNIRP publication[7].

λ (nm)	EL (J m^{-2})	EL (mJ cm^{-2})	$S(\lambda)$	λ (nm)	EL (J m^{-2})	EL (mJ cm^{-2})	$S(\lambda)$
180	2500	250	0.012	310	2.0×10^3	2.0×10^2	0.015
190	1600	160	0.019	313	5.0×10^3	5.0×10^2	0.006
200	1000	100	0.03	315	1.0×10^4	1.0×10^3	0.003
205	590	59	0.051	316	1.3×10^4	1.3×10^3	0.0024
210	400	40	0.075	317	1.5×10^4	1.5×10^3	0.002
215	320	32	0.95	318	1.9×10^4	1.9×10^3	0.0016
220	250	25	0.12	319	2.5×10^4	2.5×10^3	0.0012
225	200	20	0.15	320	2.9×10^4	2.9×10^3	0.001
230	160	16	0.19	322	4.5×10^4	4.5×10^3	0.00067
235	130	13	0.24	323	5.6×10^4	5.6×10^3	0.00054
240	100	10	0.3	325	6.0×10^4	6.0×10^3	0.0005
245	83	8.3	0.36	328	6.8×10^4	6.8×10^3	0.00044
250	70	7	0.43	330	7.3×10^4	7.3×10^3	0.00041
254	60	6	0.5	333	8.1×10^4	8.1×10^3	0.00037
255	58	5.8	0.52	335	8.8×10^4	8.8×10^3	0.00034
260	46	4.6	0.65	340	1.1×10^5	1.1×10^4	0.00028
265	37	3.7	0.81	345	1.3×10^5	1.3×10^4	0.00024
270	30	3	1	350	1.5×10^5	1.5×10^4	0.0002
275	31	3.1	0.96	355	1.9×10^5	1.9×10^4	0.00016
280	34	3.4	0.88	360	2.3×10^5	2.3×10^4	0.00013
285	39	3.9	0.77	365	2.7×10^5	2.7×10^4	0.00011
290	47	4.7	0.64	370	3.2×10^5	3.2×10^4	0.000093
295	56	5.6	0.54	375	3.9×10^5	3.9×10^4	0.000077
297	65	6.5	0.46	380	4.7×10^5	4.7×10^4	0.000064
300	100	10	0.3	385	5.7×10^5	5.7×10^4	0.000053
303	250	25	0.12	390	6.8×10^5	6.8×10^4	0.000044
305	500	50	0.06	395	8.3×10^5	8.3×10^4	0.000036
308	1200	120	0.026	400	1.0×10^6	1.0×10^5	0.00003

Next, the *Spectral Weighting Function* is described, which will be later used to compute T_{max} due to UVR originating from a polychromatic source. A derivation of the general formula for T_{max} is presented at the end of the section.

3.3 Spectral Weighting (Effectiveness) Function, $S(\lambda)$

For a monochromatic source, EL can be either determined from Table 1, or computed by interpolating those values that are already available in the table. However, in practice all the artificial sources are polychromatic (i.e., the spectral radiant power distribution function is nonzero for a range of wavelengths). In this case, the EL associated with the source can be obtained by using the continuous empirical function $S(\lambda)$ – *Spectral Weighting Function*. $S(\lambda)$ is defined for λ values in the range[29] $210 \leq \lambda \leq 400\,\mathrm{nm}$. The function represents how sensitive the human body is to UV radiation as a function of wavelength. It is also an indicator for the biological effectiveness of the radiation on the body organs, and therefore sometimes it is called *Spectral Effectiveness Function*. In terms of ELs, $S(\lambda)$ is defined as the ratio of the minimum EL to the EL at λ, that is, $S(\lambda) = \frac{EL_{min}}{EL(\lambda)}$; hence it is dimensionless. The columns in Table 1 show $S(\lambda)$ values at the corresponding wavelengths. Note that $S(\lambda)$ reaches its peak value at $270\,\mathrm{nm}$, that is, $S(\lambda)\Big|_{\lambda=270\,\mathrm{nm}} = 1$.

The continuous function $S(\lambda)$ can be used to calculate the exposure limits due to polychromatic sources; or due to monochromatic sources for radiation wavelengths different than those listed in Table 1. The function $S(\lambda)$ is given by[29]:

$$S(\lambda) = \begin{cases} 0.959^{(270-\lambda)} & \text{for } 210 \leq \lambda \leq 270\,\mathrm{nm} \\ 1 - 0.36\left(\frac{\lambda-270}{20}\right)^{1.64} & \text{for } 270 < \lambda \leq 300\,\mathrm{nm} \\ 0.3 \times 0.736^{(\lambda-300)} + 10^{(2-0.0163\lambda)} & \text{for } 300 < \lambda \leq 400\,\mathrm{nm} \end{cases} \quad (1)$$

$S(\lambda)$ is plotted in Fig. 4. The function monotonically increases for wavelengths less than 270 nm and then monotonically decreases. For λ values smaller than 270 nm, the rate of change is exponential. The rate of change of the human body sensitivity becomes maximum between 300 nm (S=0.30) and 320 nm (S=0.00126).

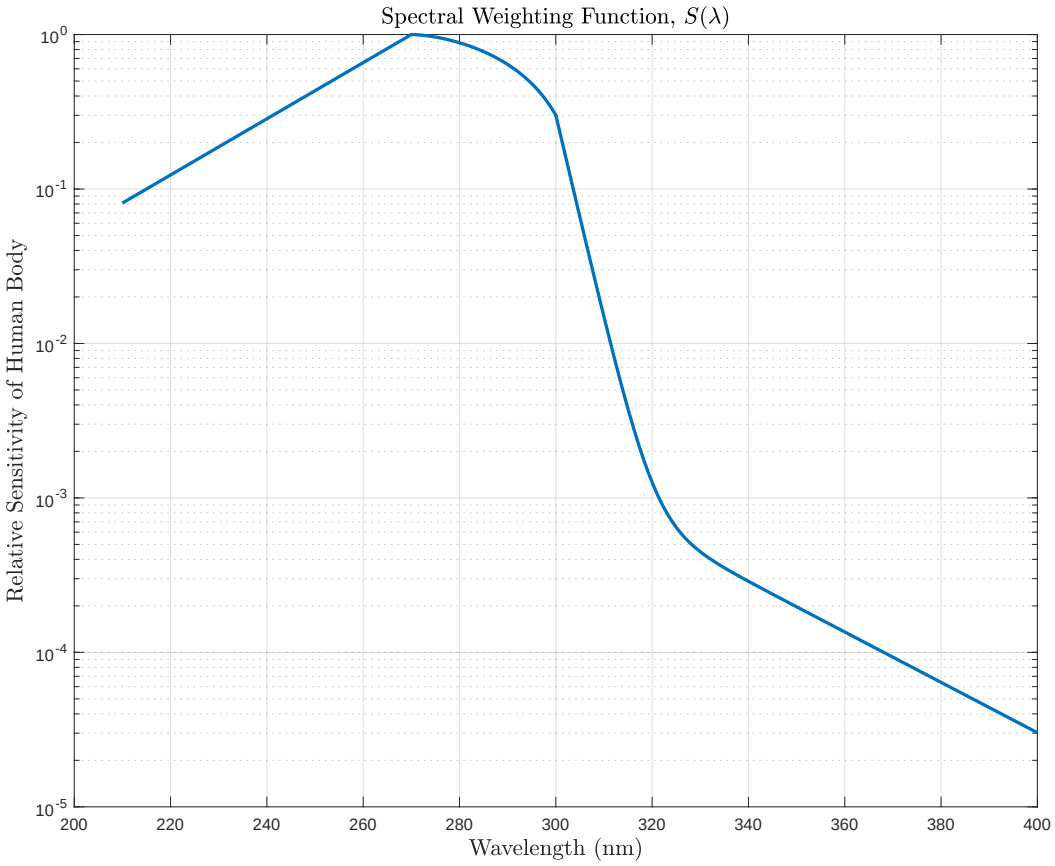

Fig. 4 Spectral weighting function, $S(\lambda)$, as given in Eq. 1, that illustrates the change in human body sensitivity due to the change in radiation wavelength within the UV spectrum

3.4 T_{max} Due to UV-C Band LED Sources

Artificial UV sources have been widely used in industry and research for a long time; examples include metal-halide (indium, thallium, etc.) mercury lamps (e.g., street lightning), xenon lamps (e.g., projectors), and quartz-halogen lamps (e.g., medical, dental applications). Recently, the Defense Advanced Research Projects Agency (DARPA) launched the Semiconductor UV Optical Source (SUVOS) program to develop miniature-size UV sources that can be integrated with tactical communication systems. Such solid-state emitters are now available on the market. A particular narrow-band LED emitter, which is potentially suitable to be employed in NLOS telecommunication links at UV-C band, is considered. Although the derivation of T_{max} is based on UV-C band LED sources, the method can be adapted to any type of incoherent UV source.

3.4.1 Definitions

3.4.1.1 SPD

The spectral power distribution function SPD describes the radiant power distribution of the spectrum. In general, UV-C emitters are polychromatic (i.e., SPD is nonzero for a continuous range of wavelengths). The normalized version of the function is of more interest when comparing two or more sources. In general, SPD is normalized either to the output power of the source or to the power level at peak wavelength—the wavelength at which the transmitted power becomes maximum. We denote normalized spectral power distribution by $\widehat{SPD}$, and use subscripts to indicate the type of normalization employed.

3.4.1.2 E_λ

At the receiver end of the UV propagation, we are interested in the amount of power incident upon a surface area, A, and how this power is distributed on the surface. The latter is given by irradiance (E) or radiant flux function. The dimension of E is power per unit area. Integrating E over A yields the incident power. For a particular system and at any point P, E is a function of system characteristics, such as the available power at the output of the source, the radiation pattern of the source, the channel between the transmitter and receiver (which includes noise in the system, single and multi-path propagations, effects due to diffraction absorption, scattering, and reflection processes along the propagating path), the location of P with respect to the transmitter, and so on. Similar to the transmitted power, the received power and irradiance have a distribution along the spectrum (spectral distribution); that is, the photon density at different wavelengths can vary (e.g., due to absorption along the propagation channel or SPD of the source). The distribution function of irradiance per unit wavelength is denoted E_λ.

For narrow-band UV-C emitters, we assume that all background noise contributing to the nonzero wavelength components is negligible due to solar-blind UVC-band. In addition, we assume the bandwidth of the source is narrow enough such that the absorption coefficient inside the channel is constant throughout the bandwidth of the source. Hence, the propagation channel does not modify the shape of the spectral distribution and the spectral distribution of the irradiance at the receiver is the same as that of the transmitter (i.e., $\widehat{SPD}_{E_\lambda} = \widehat{SPD}_{source}$).

3.4.1.3 E_{eff}

The effective irradiance, E_{eff}, is an adjusted irradiance level (power per unit area) that accounts for the radiation wavelength by using the function $S(\lambda)$. It is a measure of how damaging the associated UVR is for the skin and eye. E_{eff} is given by

$$E_{\text{eff}} = \frac{3.0 \, \frac{\text{mJ}}{\text{cm}^2}}{T_{\text{max}}} \tag{2}$$

Note that the numerator of Eq. 2 (3.0 mJ/cm^2) is the exposure limit at $270\,\text{nm}$ as given in Table 1. For safety considerations, the term E_{eff} can be taken as the equivalent irradiance level at a given point for the case when the original polychromatic source has been replaced with a fictitious monochromatic source at a wavelength of $270\,\text{nm}$. Since the EL value is well known at that wavelength, T_{max} can be calculated using Eq. 2.

3.4.2 Derivation of T_{max}

To compute T_{max} for an arbitrary location in space, SPD(λ) must be known. The effective irradiance, E_{eff}, can then be calculated by, first, weighting the spectral irradiance function E_λ at each wavelength, with $S(\lambda)$ being the weights; and then by integrating the result over the wavelength spectrum. The spectral irradiance, E_λ at some point $P(r, \phi, \theta)$ is defined in terms of spectral power distribution at P:

$$E_\lambda(r, \phi, \theta, \lambda) = \frac{\partial \left[\text{SPD}\left(r, \phi, \theta, \lambda\right)\right]}{\partial A} = \widehat{\text{SPD}}(\lambda) \, \frac{\partial \left[\text{P}_{\text{rec}}\left(r, \phi, \theta\right)\right]}{\partial A} \tag{3}$$

where ∂A is the differential surface area at point P, and normal to the direction of the incident radiant flux. The terms $\partial \text{P}_{\text{rec}}\left(r, \phi, \theta\right)$, $\widehat{\text{SPD}}\left(\lambda\right)$, and $\frac{\partial}{\partial A}\text{P}_{\text{rec}}\left(r, \phi, \theta\right)$ in Eq. 3 are, respectively, the differential received power incident upon ∂A, the normalized spectral power distribution of the source (i.e., $\int_{-\infty}^{\infty} \widehat{\text{SPD}}\left(\lambda\right) \text{d}\lambda = 1$), and the irradiance at point P (i.e., $E(r, \phi, \theta)$). When evaluating Eq. 3 it is assumed that regardless of the location of $P\left(r, \phi, \theta\right)$, the shape of $\widehat{\text{SPD}}\left(\lambda\right)$ remains the same, meaning that spectral power distribution at the output of the source is the same as the spectral distribution of the received power at P.

Consequently, if the spatial map of the function $E_\lambda(r, \phi, \theta, \lambda)$ is known over a closed surface area, A', then $P_{A'}$, the total radiant power incident upon A', can be computed:

$$P_{A'} = \oint_{A'} \int_{\lambda} E_\lambda(r, \phi, \theta, \lambda) \, \partial\lambda \, \partial A \tag{4}$$

Using Eq. 3, the effective irradiance in mW/cm^2 normalized to a monochromatic source at $270\,\mathrm{nm}$ is found to be

$$E_{\text{eff}}(r,\phi,\theta) = \int_\lambda E_\lambda(r,\phi,\theta,\lambda)\,S(\lambda)\,\mathrm{d}\lambda \tag{5}$$

$$= \frac{\partial\left[\mathrm{P}_{\text{rec}}(r,\phi,\theta)\right]}{\partial A}\int_\lambda \widehat{\mathrm{SPD}}(\lambda)\,S(\lambda)\,\mathrm{d}\lambda \tag{6}$$

$$= E(r,\phi,\theta)\int_\lambda \widehat{\mathrm{SPD}}(\lambda)\,S(\lambda)\,\mathrm{d}\lambda \tag{7}$$

Hence, the maximum exposure time T_{max} at point $P(r,\phi,\theta)$ that complies with the safety limits is

$$T_{\text{max}}(r,\phi,\theta) = \frac{3.0\,\frac{\mathrm{mJ}}{\mathrm{cm}^2}}{E_{\text{eff}}(r,\phi,\theta)} \tag{8}$$

$$= \frac{3.0\,\frac{\mathrm{mJ}}{\mathrm{cm}^2}}{E(r,\phi,\theta)\int_\lambda \widehat{\mathrm{SPD}}(\lambda)\,S(\lambda)\,\mathrm{d}\lambda} \tag{9}$$

If the incident power, $\mathrm{P}_{\text{rec},A}$, is uniformly distributed over the area A, then the irradiance is

$$E(r,\phi,\theta) = \frac{\mathrm{P}_{\text{rec},A}}{A(r,\phi,\theta)}, \tag{10}$$

where $A(r,\phi,\theta)$ is the area expressed as a function of the parameters r, ϕ, and θ.

Hemispherical lens type UV LED sources can be thought of as point UV sources, where the radiant power is confined within some critical angle[§] θ_C. Consequently, the exposure area in Eq. 10 can be defined in terms of θ_C and the radial distance from the source (recall that the radiant power incident upon the area is uniformly distributed). In this case, the exposure area $A(r,\theta_C)$ is

$$A(r,\theta_C) = \int_0^{2\pi}\int_0^{\theta_C} r^2\sin(\theta)\,\mathrm{d}\theta\,\mathrm{d}\phi \tag{11}$$

$$= 2\pi r^2(1-\cos\theta_C) \tag{12}$$

[§]The critical angle θ_C is half the vertex angle of the escape cone of the point light source.

Furthermore, the received power incident upon the area $A\left(r,\theta_C\right)$ is equal to the available power at the output of the LED source (i.e., $\mathrm{P}_{\mathrm{rec},A} = \mathrm{P}_{\mathrm{out}}$). This situation is illustrated in Fig. 5, where a UV point source is placed at the origin of a Cartesian coordinate system and the exposure area on the sphere associated with the critical angle θ_C is shown.

It is more convenient to describe the exposure area in terms of parameters of a spherical coordinate system, since the radiation is modeled as uniform in all directions. A triplet (r,ϕ,θ) of a spherical coordinate can be defined based on the Cartesian coordinates sketched in the figure such that r is the distance from the origin, ϕ is the azimuthal angle in the xy-plane, and θ is the inclination from the z-axis. Another convenient restriction that relates the system geometry and the z-axis is that the z direction is defined as the central axis of the escape cone, as shown in Fig. 5. Therefore, the coordinate system needs to be updated every time if the central axis of the escape cone is changed. This constraint is not required but simplifies the expressions. As a result, the irradiance at $P\left(r,\phi,\theta\right)$ on the sphere due to the point source at the origin is given by

$$\mathrm{E}\left(r,\phi,\theta\right) = \mathrm{E}\left(r,\theta\right) = \begin{cases} \frac{P_{\mathrm{rec},A}}{A(r,\theta)} = \frac{P_{\mathrm{out}}}{A(r,\theta_C)}, & \text{if } |\theta-\theta_C| \leq 0 \\ 0, & \text{otherwise} \end{cases} \tag{13}$$

where Eq. 13 holds if the z-axis direction coincides with the central axis of the cone. Combining Eqs. 9, 12, and 13 yields

$$T_{\max}\left(r,\theta\right) = \begin{cases} \frac{3.0\ \frac{\mathrm{mJ}}{\mathrm{cm}^2}}{\frac{\mathrm{P}_{\mathrm{rec},A}}{A(r,\theta)} \int_\lambda \widehat{\mathrm{SPD}}(\lambda) S(\lambda)\ \mathrm{d}\lambda}, & \text{if } |\theta-\theta_C| \leq 0 \\ \infty, & \text{otherwise} \end{cases} \tag{14}$$

The results indicate that $T_{\max}$ can be computed if either the received power upon area A is known through measurements, or if the available optical power at the output of the point source is known or provided by the manufacturer.

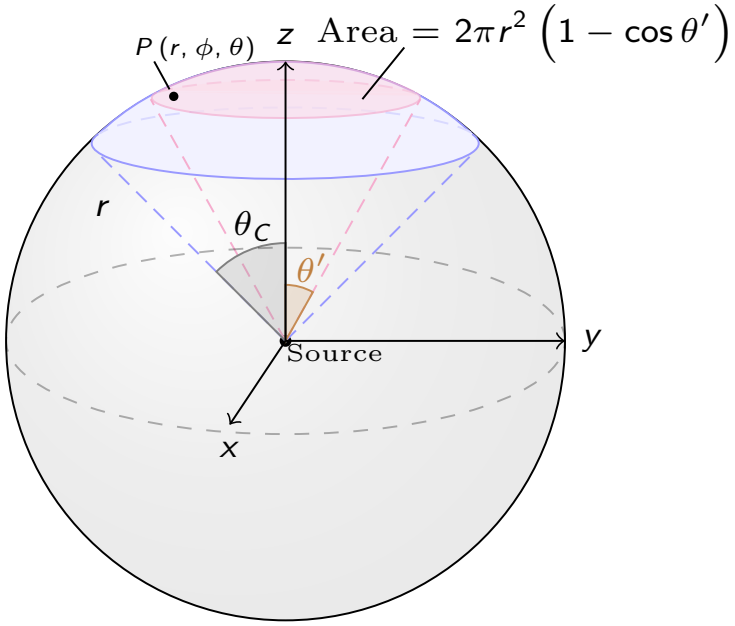

Fig. 5 The geometrical view of the system, where a point source is placed at the center of the sphere and the irradiance remains constant over the blue and red areas as long as the radiation is in the form of a circular cone

4. Application of Safety Limits for an Actual UV LED Source

One UV source module with peak wavelength at $275\,\mathrm{nm}$ (UVCLEAN275-15 from the vendor QPhotonics) is of interest for a UV communications and networking test bed that we are developing. There are two options of this model with different geometries: flat window and hemispherical lens with different angular responses. The version with the hemispherical lens provides more collimated emissions. Furthermore, the normalized radiant intensity of UVCLEAN275-15 source with the hemispherical lens option remains almost constant within the escape cone of the LED source as shown in Fig. 6. The dashed red line in the figure (data provided by the vendor) indicates how the irradiance changes as the offset angle between the source and the detector varies from -90° to 90°. The solid blue curve shows our measurement of the irradiance at $14\,\mathrm{cm}$ range from one such source by sweeping the azimuth angle from -25° to 25° with step size of 0.45°. For the measurements, the elevation angle was set to 0° and all four LED sections inside the module were radiating. The model of the irradiance meter that was used to take the measurements was the ILT77 with a $8.5\,\mathrm{mm}$ aperture sensor from International Light Technologies. For this particular measurement setup, the majority of the radiant power was found to be confined between -10° and 10° (Fig. 6); the mean and standard deviation of the normalized radiant intensity within that azimuth range were 0.92 and 0.08, respectively.

The spectral power distribution (SPD) curve of a generic UVCLEAN275-15 UV LED source provided in the datasheet is shown in Fig. 7.

We have verified with the vendor that the vertical axis corresponds to the output power normalized by the peak power. The area under the curve in Fig. 7 is calculated to be 12.0. We use this value to normalize the SPD function so that $\int_0^\infty \widehat{SDP}(\lambda)\,\mathrm{d}\lambda = 1$.

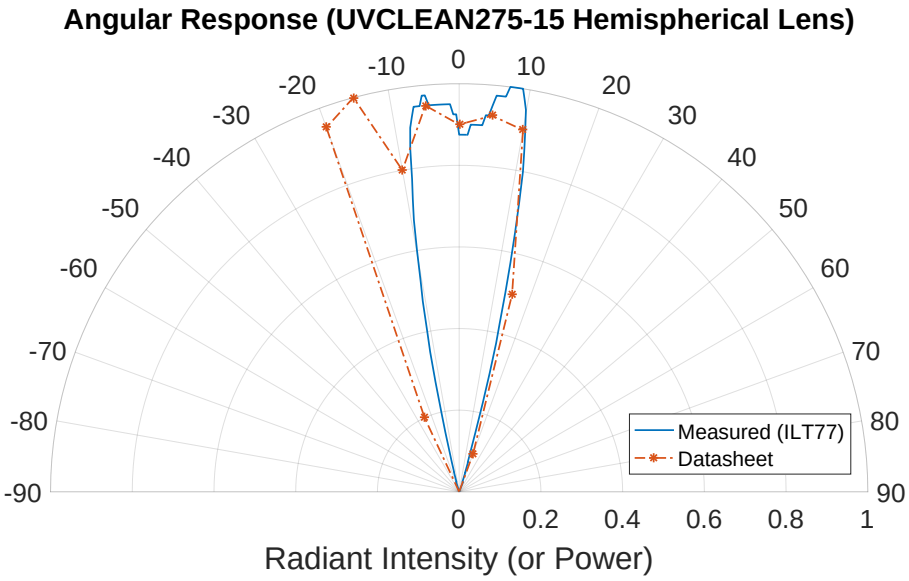

Fig. 6 The 2-D radiation pattern of the UVCLEAN275-15 source from QPhotonics. The dashed red line is reproduced from the figure on the datasheet provided by the manufacturer. The solid blue line is obtained through measurements of an actual device using ILT77 UV meter. The aperture of the meter's detector is placed $14\,\mathrm{cm}$ away from the source. In the figure, the values on the angular axis correspond to $\Delta\phi$ between the source and the aperture window, while keeping $\Delta\theta$ at 0°.

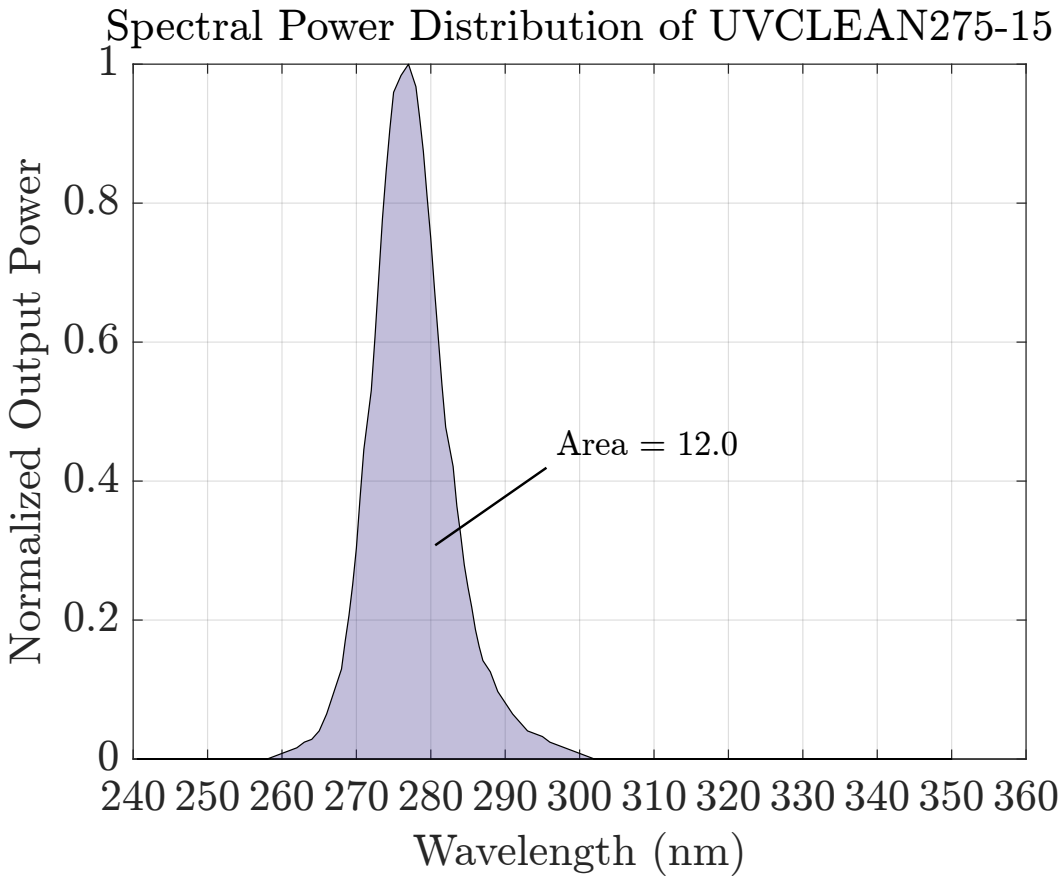

Fig. 7 Spectral power distribution of the UVCLEAN275-15 LED source. The vertical axis is normalized by the power at peak wavelength. The area under the curve corresponds to the total available power at the output, which is computed to be 12 mW.

4.1 Comparison of Measurements with Theoretical Calculations

The irradiance at a range of $14\,\mathrm{cm}$ from the source when $\phi = \theta = 0^\circ$ was measured using a ILT77 radiometer as $E_{\text{meas}}(14\,\mathrm{cm}, 0^\circ, 0^\circ) = 0.37\,\mathrm{mW/cm^2}$. The transmission of the meter's filter is given in Fig. 8. The actual irradiance at the input of the filter is found to be $0.38\,\frac{\mathrm{mW}}{\mathrm{cm^2}}$.

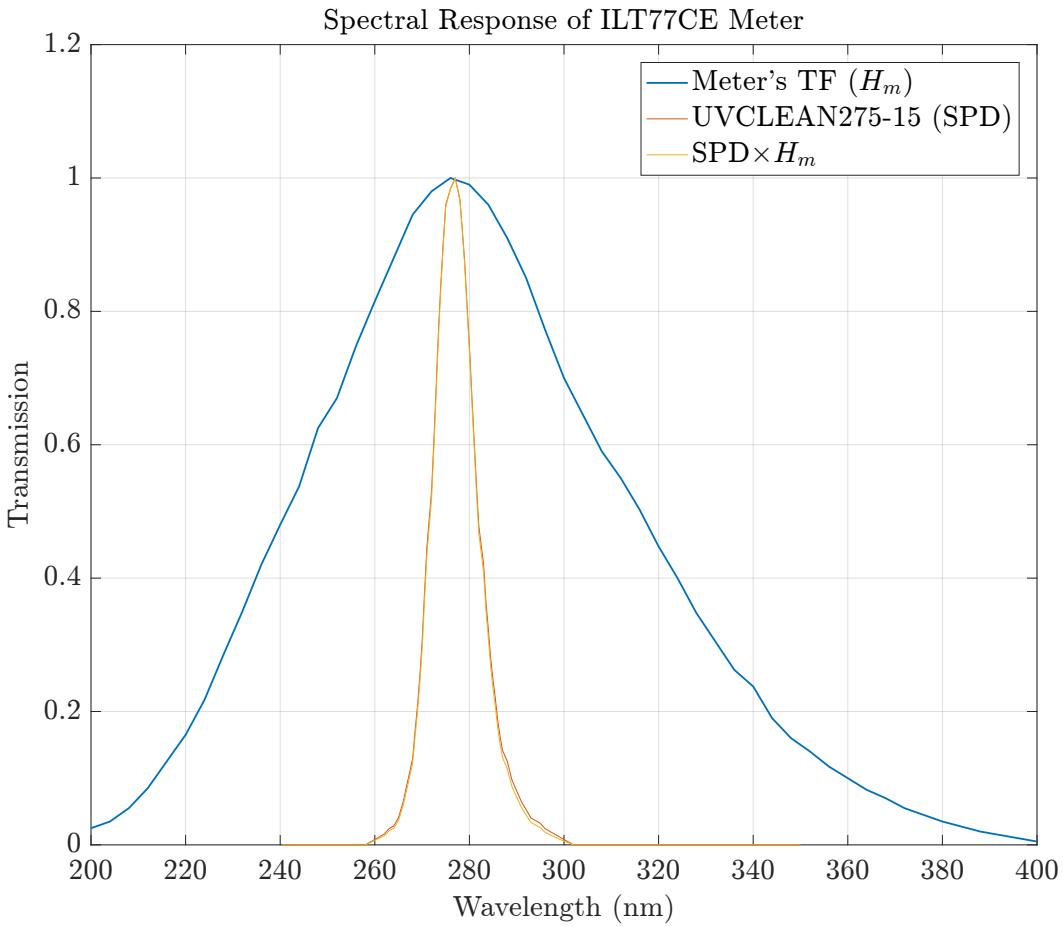

Fig. 8 The transfer function of the ILT77 filter. For this source module, the transmission of the input spectrum is close to 1.

Assuming that irradiance remains the same at any point equidistant from the source within the escape cone, the theoretical irradiance at $r = 14\,\mathrm{cm}$ can be computed for various values of P_{out} and θ_C. As shown in Fig. 9, the irradiance value is a function of θ_C. For the same output power level, for example, a 5° increase in θ_C, can reduce the irradiance for some points by more than 50%. In the datasheet of UVCLEAN275-15, the typical output power is given in the range of 10 mW–15 mW. Within that range, the $[P_{out}, \theta_C]$ pairs that yield the irradiance value of $0.38\,\frac{\mathrm{mW}}{\mathrm{cm}^2}$ are illustrated in Fig. 9 (i.e., $E_{theo} = E_{meas}$). Furthermore, if we assume that $\theta_C \simeq 13^\circ$ (see Fig. 6), then the power at the output of the source in Eq. 13 is $12\,\mathrm{mW}$.

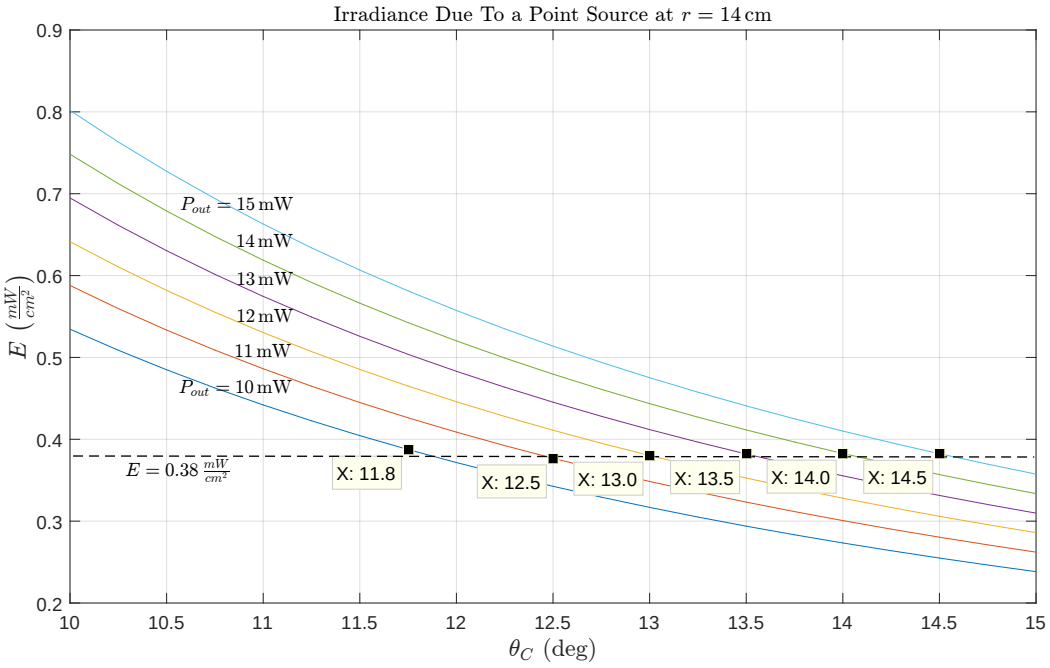

Fig. 9 The theoretical irradiance at the equidistant points from the UV source for various values of output power and θ_C values when $r = 14\,\mathrm{cm}$

4.2 Calculation of Exposure Time Limits for UVCLEAN275-15 UV LED Source

To ensure safe operation, exposure time limits must be known while working with a UV-C band LED source. In this section calculations of T_{max} are provided. In addition, we investigate how T_{max} varies as the peak wavelength of the source changes in the 255–285 nm band (see Fig. 10). We make the following assumptions for these calculations:

- A line-of-sight (LOS) channel is assumed. Scattering and absorption by obstacles near the transmitter and receiver are assumed to be minimal.
- The available power at the output of the LED source is assumed to be equal to the maximum power level given in the datasheet (i.e., $P_{out} = 15\,\mathrm{mW}$), when all the LED chips inside the module are turned on[¶]. If the actual power is different from $15\,\mathrm{mW}$, the new value of $T_{max,act}$ can be obtained by $T_{max,act} = \frac{15\,\mathrm{mW}}{P_{out,act}}\,T_{max,15\,\mathrm{mW}}$.

[¶]There are four LED chips in UVCLEAN275-15.

- The lens on the package is hemispherical and the output power is uniformly distributed between -15° and 15°, ($\theta_C = 15^\circ$). For other values of θ_C, $T_{max,act}$ can be computed using: $T_{max,act} = \frac{1-\cos(\theta_C)}{1-\cos(15^\circ)}\, T_{max,\theta_C=15^\circ}$.
- The UV LED radiation pattern is approximated by a circular cone shape.
- The results show the exposure time limits $T_{max}(r)$ for an observer at the point $P(r, \phi, \theta)$, where r is the distance from the source, ϕ is the azimuth angle in the same plane, whose normal vector is the central axis of the radiation (escape cone), and θ is the elevation angle from the central axis of the escape cone. Note that by Eq. 14, θ must satisfy $|\theta \leq \theta_C|$, otherwise $T_{max}(r) = \infty$.

The following relationships can be obtained among the time limits for various peak wavelengths: $T_{270\,\mathrm{nm}} \simeq 1.03T_{275\,\mathrm{nm}} \simeq 1.08T_{265\,\mathrm{nm}} \simeq 1.14T_{280\,\mathrm{nm}} \simeq 1.26T_{260\,\mathrm{nm}} \simeq 1.33T_{285\,\mathrm{nm}} \simeq 1.53T_{255\,\mathrm{nm}}$. Recall that these relationships hold only for the particular spectral distribution function given in Fig. 7 with the corresponding peak wavelength. Exposure time limits for sources with different peak wavelengths are listed in Table 2.

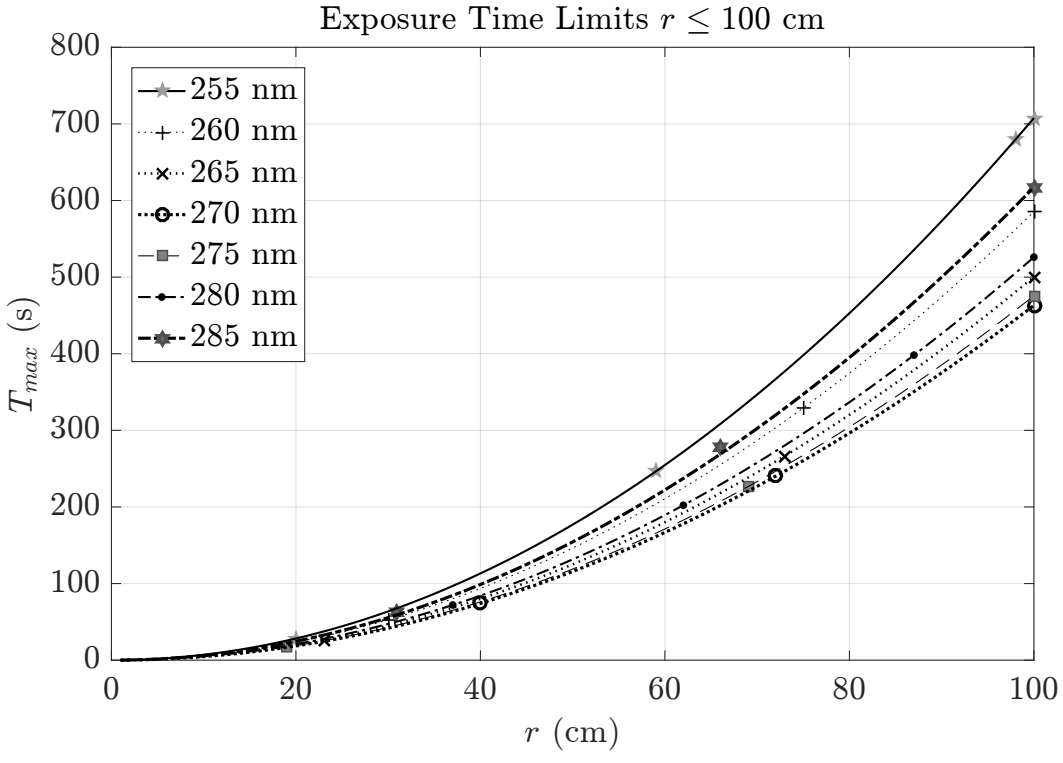

(a)

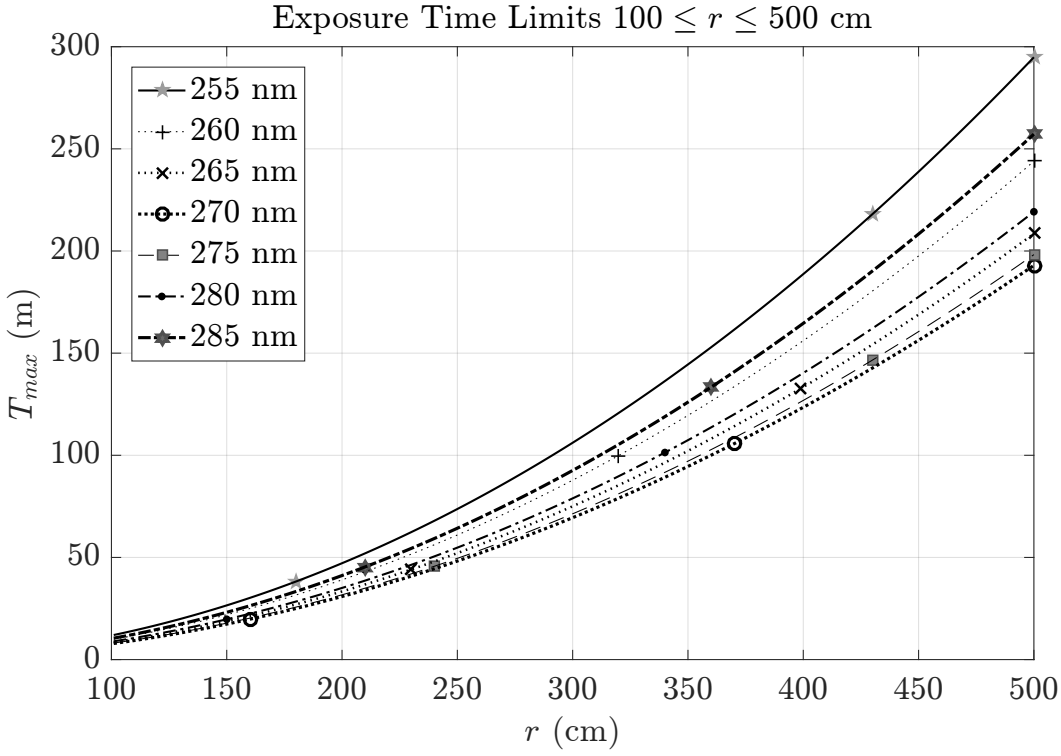

(b)

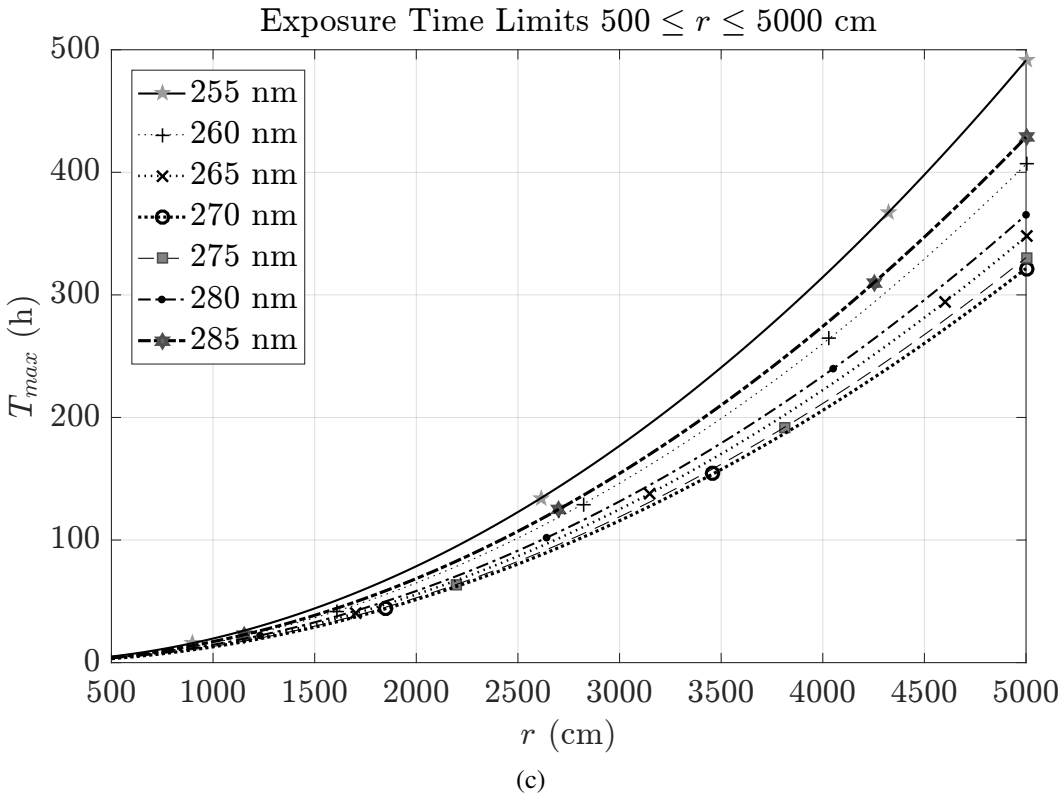

(c)

Fig. 10 Exposure time limits due to sources that have the spectral distribution shown in Fig. 7 but having different peak wavelengths

Table 2 Exposure time limits for sources with different peak wavelengths. It is assumed that each source has the same SPD function as that shown in Fig. 7, but with the peaks at different points on the wavelength axis. The columns r and T_{λ_0}, respectively, correspond to the radial distance from the source in cm, and maximum allowable exposure time, where λ_0 is the peak wavelength.

r (cm)	$T_{255\,\mathrm{nm}}$	$T_{260\,\mathrm{nm}}$	$T_{265\,\mathrm{nm}}$	$T_{270\,\mathrm{nm}}$	$T_{275\,\mathrm{nm}}$	$T_{280\,\mathrm{nm}}$	$T_{285\,\mathrm{nm}}$
1	.07 s	.06 s	.05 s	.05 s	.05 s	.05 s	.06 s
5	1.8 s	1.5 s	1.3 s	1.2 s	1.2 s	1.3 s	1.5 s
10	7.1 s	5.9 s	5.0 s	4.6 s	4.8 s	5.3 s	6.2 s
17	20.4 s	16.9 s	14.5 s	13.4 s	13.7 s	15.2 s	17.8 s
25	44.2 s	36.6 s	31.3 s	28.9 s	29.7 s	32.9 s	38.6 s
40	1.9 m	1.6 m	1.3 m	1.2 m	1.3 m	1.4 m	1.6 m
60	4.2 m	3.5 m	3.0 m	2.8 m	2.9 m	3.2 m	3.7 m
80	7.5 m	6.2 m	5.3 m	4.9 m	5.1 m	5.6 m	6.6 m
100	11.8 m	9.8 m	8.3 m	7.7 m	7.9 m	8.8 m	10.3 m
150	26.5 m	22.0 m	18.8 m	17.4 m	17.8 m	19.7 m	23.1 m
180	38.2 m	31.6 m	27.0 m	25.0 m	25.7 m	28.4 m	33.3 m
210	52.0 m	43.0 m	36.8 m	34.0 m	35.0 m	38.7 m	45.4 m
250	73.7 m	61.0 m	52.1 m	48.2 m	49.6 m	54.8 m	64.3 m
290	99.2 m	82.1 m	70.1 m	64.9 m	66.7 m	73.7 m	86.5 m
340	2.3 h	1.9 h	1.6 h	1.5 h	1.5 h	1.7 h	2.0 h
400	3.1 h	2.6 h	2.2 h	2.1 h	2.1 h	2.3 h	2.7 h
500	4.9 h	4.1 h	3.5 h	3.2 h	3.3 h	3.7 h	4.3 h
600	7.1 h	5.9 h	5.0 h	4.6 h	4.8 h	5.3 h	6.2 h
750	11.1 h	9.1 h	7.8 h	7.2 h	7.4 h	8.2 h	9.6 h
850	14.2 h	11.7 h	10.0 h	9.3 h	9.5 h	10.6 h	12.4 h
1000	19.7 h	16.3 h	13.9 h	12.9 h	13.2 h	14.6 h	17.1 h
1200	28.3 h	23.4 h	20.0 h	18.5 h	19.0 h	21.0 h	24.7 h
1500	44.2 h	36.6 h	31.3 h	28.9 h	29.7 h	32.9 h	38.6 h
2000	78.6 h	65.0 h	55.6 h	51.5 h	52.9 h	58.5 h	68.6 h
5000	491.4 h	406.6 h	347.5 h	321.6 h	330.4 h	365.3 h	428.6 h

5. Conclusion

In this report the safe operation of incoherent UV LED sources at the UV-C band is investigated. Exposure limits for both the skin and the eye are considered. By assuming an LOS channel and the SPD function that describes the radiant power distribution along the spectrum, the spectral irradiance is calculated from which the maximum theoretical exposure time limit is computed. Furthermore, the maximum exposure time limits are also computed for a specific UV LED source that is being used for a UV communications and networking experimentation test bed based on measured data. These exposure time limits for ranges up to 50 m for wavelengths from 255 nm to 285 nm are presented. It should be noted that similar approaches can be pursued for other types of UV LED sources with different transmit power levels and wavelengths. The results in this report can readily be used by researchers and technicians using such devices to ensure their safety and the safety of others within range of these devices.

6. References

1. Xu Z, Sadler BM. Ultraviolet communications: Potential and state-of-the-art. IEEE Communications Magazine. 2008;46(5):67–73.

2. Xu Z, Ding H, Sadler BM, Chen G. Analytical performance study of solar blind non-line-of-sight ultraviolet short-range communication links. Opt. Lett. 2008;33(16):1860–1862.

3. Chen G, Xu Z, Sadler BM. Experimental demonstration of ultraviolet pulse broadening in short-range non-line-of-sight communication channels. Optics Express. 2010;18.

4. Drost RJ, Moore TJ, Sadler BM. UV communications channel modeling incorporating multiple scattering interactions. J. Opt. Soc. Am. A. 2011;28(4):686–695.

5. de Gruijl F, Leun J. Environment and health: 3. ozone depletion and ultraviolet radiation. Canadian Medical Association Journal. 2000;163(7):851–855.

6. UV Workers' Protection Statement; 2010 [accessed 2017 May]. http://www.icnirp.org/cms/upload/publications/ICNIRPUVWorkersHP.pdf.

7. ICNIRP Guidelines on Limits of Exposure to Ultraviolet Radiation of Wavelengths Between 180 nm and 400 nm; 2004 [accessed 2017 May]. http://www.icnirp.org/cms/upload/publications/ICNIRPUV2004.pdf.

8. Stanford Solar Center: UV Light [accessed 2018 May]. http://solar-center.stanford.edu/about/uvlight.html.

9. Imagine the Universe!; 2013 [accessed 2018 May]. https://imagine.gsfc.nasa.gov/science/toolbox/emspectrum2.html.

10. Wehrli C. Extraterrestrial solar spectrum. Physikalisch-Meteorologisches Observatorium + World Radiation Center (PMO/WRC) Davos Dorf. (615).

11. Roy C, Gies H, Lugg D, Toomey S, Tomlinson D. The measurement of solar ultraviolet radiation. Mutation Research/Fundamental and Molecular Mechanisms of Mutagenesis. 1998;422(1):7–14.

12. Van Der Leun JC. The ozone layer. Photodermatology, Photoimmunology & Photomedicine. 2004;20(4):159–162.

13. Gilchrest BA, Eller MS, Geller AC, Yaar M. The pathogenesis of melanoma induced by ultraviolet radiation. New England Journal of Medicine. 1999;340(17):1341–1348.

14. Svobodova A, Walterova D, Vostalova J. Ultraviolet light induced alteration to the skin. Biomedical papers of the Medical Faculty of the University Palacky, Olomouc, Czechoslovakia. 2006;150(1).

15. Sayre RM, Dowdy JC, Shepherd J, Sadiq I, Baqer A, Kollias N. Vitamin D -vs- erythema: effects of solar angle & artificial sources. In: Holick MF, Jung EG, editors. Biologic Effects of Light 1998. Proceedings of the Fifth International Arnold Rikli Symposium on the Biologic Effects of Light; 1998 Nov 1–3; Basel, Switzerland. Boston, MA: Springer US; 1999. p. 149–152.

16. Madronich S, McKenzie RL, Bjorn LO, Caldwell MM. Changes in biologically active ultraviolet radiation reaching the earth's surface. Journal of Photochemistry and Photobiology B: Biology. 1998;46(1):5–19.

17. McKenzie RL, Aucamp PJ, Bais AF, Bjorn LO, Ilyas M, Madronich S. Ozone depletion and climate change: impacts on UV radiation. Photochem. Photobiol. Sci. 2011;10(2):182–198.

18. Hockwin O, Kojima M, Muller-Breitenkamp U, Wegener A. Lens and cataract research of the 20th century: A review of results, errors and misunderstandings. Developments in Ophthalmology. 2002;35:1–11.

19. Ayala MN, Soderberg PG. Reversal of reciprocity failure for UVR-induced cataract with vitamin E. Ophthalmic Research. 2005;37(3):150–155.

20. Aubin F. Mechanisms involved in ultraviolet light-induced immunosuppression. European Journal of Dermatology: EJD. 2003;13(6):515–523.

21. Parrish J, Jaenicke K, Anderson R. Erythema and melanogenesis action spectra of normal human skin. Photochemistry and photobiology. 1982;36(2):187–191.

22. Ziegler A, Jonason A, Leffell D, Simon J, Sharma H, Kimmelman J, Remington L, Jacks T, Brash D. Sunburn and p53 in the onset of skin cancer. Nature. 1994;372(6508):773–776.

23. UV Radiation Guide, NAVY Environmental Health Center; 1992 [accessed 2017 May]. http://www.med.navy.mil/sites/nmcphc/Documents/policy-and-instruction/ih-ultraviolet-radiation-technical-guide.pdf.

24. Decoster D, Harari J. Optoelectronic sensors. London, UK: ISTE; 2009.

25. Kvam E, Tyrrell R. Induction of oxidative DNA base damage in human skin cells by UV and near visible radiation. Carcinogenesis. 1997;18(12):2379–2384.

26. Tornaletti S, Pfeifer G. UV damage and repair mechanisms in mammalian cells. BioEssays: news and reviews in molecular, cellular and developmental biology. 1996;18(3):221–228.

27. Vecchia P et al. Protecting workers from ultraviolet radiation. (vol. 14).

28. Berg-Perier M, Cederblad A, Persson U. Ultraviolet radiation and ultra-clean air enclosures in operating rooms. The Journal of Arthroplasty. 1997;7(4):457–463.

29. Wester U. Analytic expressions to represent the hazard ultraviolet action spectrum of ICNIRP & ACGIH. Radiation Protection Dosimetry. 2000;91(1-3):231–232.

List of Symbols, Abbreviations, and Acronyms

ACGIH	American Conference of Governmental Industrial Hygienists
ARL	US Army Research Laboratory
DARPA	Defense Advanced Research Projects Agency
DNA	deoxyribonucleic acid
EL	exposure limit
EM	electromagnetic
EUV	extreme ultraviolet
ICNIRP	International Commission on Non-Ionizing Radiation Protection
IEC	International Electrotechnical Commission
ILO	International Labour Organization
LED	light-emitting diode
LOS	line-of-sight
NIOSH	National Institute for Occupational Safety and Health
NLOS	non-line-of-sight
SPD	spectral power distribution
SUVOS	Semiconductor Ultraviolet Optical Source
UV	ultraviolet
UVR	ultraviolet radiation
VL	visible light

1 (PDF)	DEFENSE TECHNICAL INFORMATION CTR DTIC OCA
2 (PDF)	DIR ARL IMAL HRA RECORDS MGMT RDRL DCL TECH LIB
1 (PDF)	GOVT PRINTG OFC A MALHOTRA
4 (PDF)	ARL RDRL CIN D M WEISMAN RDRL CIN T H ARSLAN F DAGEFU R DROST